ACTA METALLURGICA SLOVACA
2025, VOL. 31, NO. 3, 171-180

RESEARCH PAPER

Effects of Arc Quenching on the Surface Hardness of Medium Carbon Steel

Pham Son Minh[1], Van-Thuc Nguyen[1], Tronghieu Nguyen[1], Vinh Tien Nguyen[1], Nguyen Ho[2,]*

[1] HCMC University of Technology and Education, Ho Chi Minh City 71307, Viet Nam;
[2] HCMC University of Technology and Education, Faculty of Mechanical Engineering, Ho Chi Minh City 71307, Viet Nam

*Corresponding author: hon.ncs@hcmute.edu.vn, tel.: +84977951638, Faculty of Mechanical Engineering, HCMC University of Technology and Education, 71307, Ho Chi Minh City, Viet Nam

Received: 17.07.2025
Accepted: 28.07.2025

ABSTRACT
This work investigates the surface hardness after arc quenching S45C steel with a convex surface, including arc length, current intensity, travel speed, gas flow rate, and pulse duration. The intensity of the current mostly determines the surface hardness. Interestingly, the convex surface shows an impressive 108% increase from its initial hardness of 182 HV. Increased heat input at high current intensity may be the cause of the overheating and melting phenomena, as well as the decreased hardness. Surface hardness generally increases with increases in gas flow rate, resulting from an enhanced gas cooling rate. Similar to the gas flow rate, surface hardness rises with TIG gun travel speed. In addition, the convex surface hardness's Taguchi prediction value is 359.6 HV. The ideal parameters are 90 A for the current intensity, 2.5 mm for the arc length, 12 l/min for the gas flow rate, 200 mm/min for the travel speed, and 0.7 s for the pulse duration. In addition, 3D surface plots were used to evaluate the degree of interaction between parameters. For the S45C convex surface, the maximum case depth of the arc quenching is 3500 µm. The hardened area, the heat-affected area, and the base substrate are the three regions of the arc quenching sample's microstructure.

Keywords: surface hardness, convex shape, current intensity, microstructure, heat treatment

INTRODUCTION
Surface heat treatment is a method that significantly changes the microstructure [1] and mechanical properties of the steel surface to improve its characteristics and performance [2]. This method is performed by heating the surface to a certain temperature threshold and rapidly cooling it to form a martensite phase, thereby increasing the surface hardness of the steel [3]. In the study of [4], AISI 1020 material was used to conduct experiments on the influence of heat treatment on the mechanical properties of the material. The material was heated to 727°C and then cooled in different environments, including water, air, and sand. The results showed that heat treatment significantly affected the mechanical properties of the material. In particular, the hardness of the material changed after heat treatment with an increase of 1.59 times compared to the initial hardness (357 HRB/224 HRB) when heat-treated and cooled in water (quenched in water). In addition, the appearance of martensite structure in the microstructure was examined by electron microscopy. The material grain structure becomes smaller and finer than the original grain size obtained.
Table 1 is the result of some previous studies of different surface hardening methods. The surface after treatment has a higher hardness than the original, and its depth is several millimeters, sufficient to be used without altering the toughness of the inner layer of the steel, as the heat treatment process does not affect the inside [5]. The study of Kulkarni et al. [6] compared the hardness and toughness of AISI 1020 steel using three methods: induction hardening, flame hardening, and 2-3mm carburizing for AISI 1020 steel used in the automotive industry. The results showed a good improvement in hardness and toughness. The structure of the flame-hardened surface was similar to that of the volume-hardened steel sample, and it was composed of two phases, ferrite and bainite. However, the internal structure of the flame-hardened sample was similar to the original structure of the steel material, so it still maintained its toughness. This helped the surface to be both hardened and still ensure its toughness. Therefore, the surface quenching method is technically very efficient while still maintaining good economic viability since it requires minimal energy to perform the quenching process. There are many different surface quenching techniques including: flame quenching, laser quenching, electron beam quenching, induction quenching and arc quenching [7-11].

Table 1 Research results of some surface quenching methods of steel materials

No	Refs.	Method quenching	Parameters	Hardness improvement compared to original	Depth of case hardening
1	[7]	Laser quenching	40CrMnMo7 steel; length 150 mm, 200 mm, 250 mm; Spot Laser(mm): 4 mm, 5 mm, 7 mm; T: 1150 ^{0}C, 1250 ^{0}C, 1350 ^{0}C; travel speed: 3, 5, 7 mm/s	Increased by 3.48 times	0.4 mm - 1.4mm
2	[8]	Flame quenching	12Cr steel; The maximum surface temperature T S,max was varied from 750 ^{0}C to 1240 ^{0}C at surface of steel	Increased by 2.2 times	10 mm - 18 mm
3	[9]	Electron beam quenching	C45 steel; 60 kV for acceleration voltage, 1.589 m/min for the scanning speed which was limited by shaft diameter and the speed of turntable, 25 mA, 26 mA, 27 mA, 28 mA and 29 mA respectively for beam current	Increased by 4-5 times	0.3 mm - 0.45 mm
4	[10]	Induction quenching	Medium carbon steel, The material was austenitized at temperature of 900 ^{0}C through induction heating on one of its surfaces for 3 s^{-1}, cooling with oil	Increased by 1,8 times	7.7 mm
5	[12]	Arc quenching	Use 20, 40, 65G and U8 steel. Travel speed from 0.01 m/s - 5m/s; Current intensity was 100 A - 250 A	Increased by 3.57 times	0.4 mm
6	[13]	Arc quenching	AISI 4340 steel; current intensity was 80 A, 100 A, 120 A, 140A; travel speed was 6 cm/min, 9 cm/min, 12 cm/min, 15 cm/min	Increased by 2.88 times	1.5 mm - 3 mm

DOI: https://doi.org/10.36547/ams.31.3.2220

Among them, flame hardening has the largest hardening depth, but the hardness improvement is relatively low. This is similar to the induction hardening method. Laser hardening and electron beam hardening seem to be identical in that they use extremely hot energy sources to raise the surface temperature very quickly and then cool the part itself. This method gives very high hardness, but the hardening depth is low because they are performed in a very short time.

Similar to the two methods of laser quenching and electron beam quenching. The method of quenching with electric arc energy is a method that uses the extremely strong energy source of the arc to heat the surface of the steel material very quickly, and then rapid cooling by the quenched part itself without the need for rapid cooling agents such as oil, water, or salt [14]. The advantages of this method are that the process is fast and ensures productivity, and especially the equipment is very easy to use, so the cost is low [15]. Many different scientists have used this method to carry out their research in recent years.

Mikheev et al. [12] investigated the arc-quenching process of the carbon steel by using a constricted electric arc. This study surveyed the arc quenching ability of the low-carbon, medium-carbon, and high-carbon steel. The case depth of the medium-carbon and high-carbon steel is about 500 µm. In addition, the highest microhardness of 7.3–9.5 GPa of the medium-carbon steel could be obtained when the travel speed of the arc touch is 70–90 mm/s. Also in 2017, Kumar et al. [13] used the arc energy generated from the TIG torch to modify the surface of AISI 4340 steel. The work varied the two input parameters, current intensity and travel speed. In addition, the study also focused on evaluating the 30% overlap of the quenching width of the previous layer, as well as the use of multiple quenching for a surface. The results showed a significant increase in surface hardness, reaching 720 HV for a single quench and 445 HV for multiple quenches compared to the initial 250 HV.

The surface hardness after quenching depends on the heat input. The parameters that affect the heat input include current intensity and travel speed. Kumar et al. [16] used electric arc energy to improve the tensile and fatigue properties of AISI 4340 steel. The author of the article changed 2 parameters affecting the input heat and current intensity (from 80-140 A) and travel speed (6-15 cm/min). The results of the article showed that the depth of the surface layer with improved properties ranged from 2.5mm to 6.7mm, depending on the input heat. The combined heat control of the input heat between the 2 parameters of current intensity and travel speed facilitates the creation of the desired microstructure with a combination of martensite and banite matrix. Increasing the input heat reduces the yield limit but increases the ductility and impact toughness of the steel after quenching. The optimal travel speed at 9-12 cm/min will increase the highest ductility and toughness. It also increases fatigue life by forming compressive residual stress at 200-25 MPa assessed at a depth of 0.2-1mm.

E.N. Safonov and M.V. Mironova [17] used arc energy to quench the surface of low-carbon steel. The steel grades used were 09G2, 20L, and 20FL with a carbon concentration of about 0.2%. The input parameters for the investigation were travel speed from 80-180 m/h, current intensity 180-330A, and an overlap in the quenching zone was 30-50%. The results of the study showed that the depth of the hardened zone ranged from 0.7-1mm, the microhardness ranged from 3900 to 8800 MPa, and the structure of the hardened zone had martensitic-austenitic grains.

Like other methods, after the surface quenching process, the surface hardness will be improved, and the mechanical properties will change. The reason for this change is the appearance of martensite, bainite and other phases. Kurma et al. [18] studied the properties of AISI 8620 steel through the arc quenching process, focusing on the thermal and metallurgical properties. Here, the authors only investigated the change in current intensity (from 70 – 200A) and the overlap between the layers (overlapping 1/3 width compared to the previous layer). The maximum depth of the metal layer after quenching, which increased in hardness, reached from 2.5 mm to 5.5 mm, depending on the current intensity. The microstructure of the arc quenched samples can be divided into three zones, including the hardening zone, the heat affected zone (HAZ), and the base metal. The results showed impressive hardness, with the highest hardness achieved at 492 HV compared to 210 HV of the unquenched sample. They also showed that with the presence of martensite and bainite, the wear resistance, fatigue strength, and corrosion resistance of the quenched steel were enhanced.

In addition, Dewangan et al. [19] performed metal arc welding of 4 pairs of AISI 1020 materials. After welding, 1 sample was retained, the remaining 3 samples were heat treated by 3 different methods: oil quenching, water quenching and steel annealing. The results showed that heat treatment in the weld zone (molten metal zone) only improved the hardness by about 5% when increasing from 73.2 HRB to 77 HRB for water quenching and 76 HRB for oil quenching. This can prove that quenching does not significantly improve the weld quality. Therefore, electric arc quenching is a very effective method to improve the surface hardness of S45C steel.

However, arc quenching studies are not frequently performed. Further reports are needed to clarify the influence of arc quenching characteristics such as arc length, current intensity, travel speed, and gas flow. In particular, since many factors can affect the arc quenching process, optimization tools should be considered to find the optimal parameter set as well as to learn more about the interaction between the above factors. In addition to flat surfaces, convex surfaces also need to be further studied because they are common surfaces, such as hollow shafts. The heat transfer process occurring on convex surfaces will be different from that occurring on flat surfaces, leading to changes in surface hardness [20]. Dong Ju Kim et al. [21] conducted a study on heat transfer on three different types of surfaces, including convex, concave, and flat. The experimental study investigated the convective thermal conductivity of the scanning beam acting on the surfaces. The results show that the curved surface had a better heat transfer rate from the scanning beam than the flat surface. Meyghani and Awang [22] investigated the thermal and stress behavior when using friction stir welding on two flat and curved surfaces of AA6061-T6 alloy material. The results show that the flat surface always had a higher temperature than the curved surface from 50 °C to 80 °C, and the stress of the curved surface was always lower than that of the flat surface under the same conditions. Therefore, it is necessary to study samples with convex surfaces during the arc quenching process to expand its application in industry.

This study attempted to examine the effects of carbon steel characteristics under various arc quenching conditions of the convex surface. The effects of gas flow rate (GFR), travel speed (Tr-S), Current intensity (Cr-I), and arc length (Ar-L) on the carbon steel's hardness are investigated. Additionally, the arc quenching sample's microstructure is examined. The optimization process via the Taguchi method is also discussed. The industry-available tungsten inner gas (TIG) and computer numerical control (CNC) machines create the arc quenching apparatus. The study's findings could enhance our understanding of this heat treatment method and facilitate its use in commercial applications.

MATERIAL AND METHODS

Material and heat treatment equipment

Medium carbon steel S45C is a type of steel widely used in industrial machines. Commonly used parts are gears, shafts, shaft joints...... These parts need to be surface hardened to improve surface mechanical properties and surface wear resistance. **Table 2** shows the chemical composition parameters of medium carbon steel S45C in the electric arc quenching test.

Table 2 Chemical composition of S45C steel samples**.**

Weight %	C	Si	Mn	P	S	Ni	Cr
S45C	0.42-0.50	0.17-0.37	0.5-0.8	0.035 max	0.035 max	0.25 max	0.25 max

The surface quenching process by electric arc is carried out with the equipment and implementation as shown in **Fig. 1**.

Fig. 1a shows the shape and size of the experimental part. The experimental part has a length of 180 mm, a width of 50 mm, and a maximum height of 35 mm. The convex surface used for the experimental survey has a radius of 60 mm, and the thickness of the part is 6 mm. When experimenting with an electric arc, each part will survey three different experimental cases, as shown in three red lines in **Fig. 1a**. These lines are 12.5mm apart to avoid thermal effects on the position that has been performed. **Fig. 1b** is a detailed image after completing the surface quenching process. **Fig. 1c** is an image when preparing to start the process. In the electric arc quenching experiment, the arc will be created from the TIG head (**Fig. 1c**) of the Jasic TIG welding machine, manufactured in Vietnam. To control the quenching process with a convex shape, the CNC machine has been used in this case. The machine has three linear moving axes and 1 TIG head rotating axis, ensuring that the TIG head is always perpendicular to the surface of the experimental part.

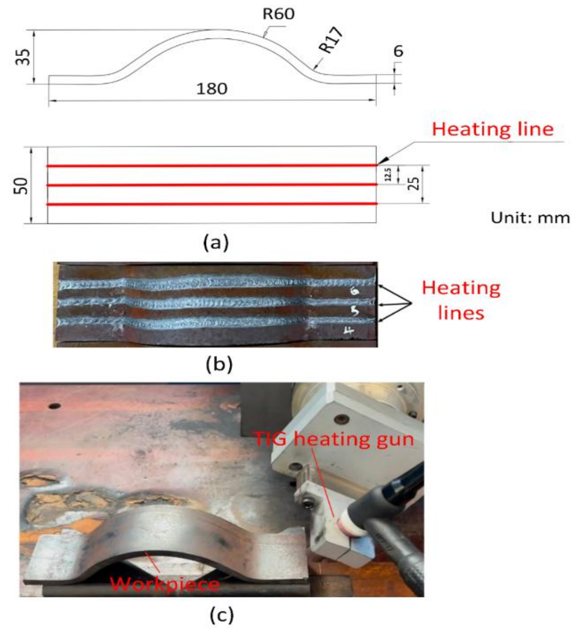

Fig. 1 Steel sample and arc quenching technique: (a) S45C steel shape with convex surface, (b) Hardening surface, and (c) arc quenching machine with TIG gun and CNC machine

Parameters of the arc quenching

The temperature field model in a moving TIG arc was proposed by Nguyen et al. [23] with a double elliptical power density and has been demonstrated in many previous studies [12, 13, 16, 17]. The Cr-I is a very important parameter to create a heat source to perform the quenching process [24]. This study investigates the Cr-I levels of 90 A, 100 A, 110 A, 120 A, 130 A with the same survey range but the step change is 10A shorter than the 20A step of the [18] study to find a clearer level of influence. The distance from the TIG head to the surface of the part (Ar-L) is an extremely important parameter, it directly affects the electric arc generation process. If this distance is less than 1mm, it is very easy to not generate light and often sticks to the part because it is too close. If it is greater than 3 mm, this is a quite far distance, it is easy not to generate electric arc and if it does, it will create a rather weak arc. Therefore, this study will be conducted at the levels of 1 mm, 1.5 mm, 2 mm, 2.5 mm and 3 mm. Pulse duration is also an important parameter to create arc energy. If the pulse time is too long, it will cause overheating [25], so in this study, the levels of 0.3 s, 0.5 s, 0.7 s, 0.9 s, 1.1 s will be selected. Unlike the above 3 parameters that affect the arc heat generated from the TIG head, the Tr-S parameter affects the heat input of the part. According to the study of [13], increasing the Tr-S will reduce the amount of heat absorbed, reducing the area of the deformed zone. On the contrary, when the Tr-S is reduced, the heat flow will increase, increasing the area of the deformed zone. However, when the amount of heat increases, the rapid cooling process will slow down, reducing the amount of martensite formed, so the surface hardness can be reduced. This study will investigate the levels of 100 mm/min, 150 mm/min, 200 mm/min, 250 mm/min, and 300 mm/min. In addition, the GFR for the TIG process also affects the rapid cooling rate. Therefore, the study considers different gas flow rates, including: 11.5 l/min, 12 l/min, 12.5 l/min, 13 l/min, 13.5 l/min. The specific experimental parameters are presented in **Table 3**. Besides, the experimental voltage was fixed at 80V.

Table 3. The factors and five levels

Design variables	Unit	Level 1	Level 2	Level 3	Level 4	Level 5
The arc length	mm	1	1.5	2	2.5	3
The current intensity (Cr-I)	A	90	100	110	120	130
The travel speed	mm/min	100	150	200	250	300
The gas flow rate (Q)	l/min	11.5	12	12.5	13	13.5
Pulse duration (F)	s	0.3	0.5	0.7	0.9	1.1

This study will conduct two different experimental methods. The first method will investigate the influence of each parameter on the hardness of the steel surface after quenching, which is called a univariate investigation method. The specific parameters of the experiment are shown in **Table 4**.

Table 4. Parameters of the arc process in the surface quenching test.

<table>
<tr><th>No.</th><th>Intensity (A)</th><th>Arc length (mm)</th><th>Q l/min)</th><th>F (mm/min)</th><th>Pulse duration (s)</th><th>Average Surface hardness (HV)</th></tr>
<tr><td>1</td><td>90</td><td rowspan="5">1.5</td><td rowspan="10">12.5</td><td rowspan="15">150</td><td rowspan="20">0.5</td><td>351.6</td></tr>
<tr><td>2</td><td>100</td><td>373.4</td></tr>
<tr><td>3</td><td>110</td><td>378.6</td></tr>
<tr><td>4</td><td>120</td><td>344.6</td></tr>
<tr><td>5</td><td>130</td><td>343.4</td></tr>
<tr><td>6</td><td rowspan="20">110</td><td>1</td><td>365.2</td></tr>
<tr><td>7</td><td>1.5</td><td>332.2</td></tr>
<tr><td>8</td><td>2</td><td>321.8</td></tr>
<tr><td>9</td><td>2.5</td><td>300.6</td></tr>
<tr><td>10</td><td>3</td><td>309.6</td></tr>
<tr><td>11</td><td rowspan="15">1.5</td><td>11.5</td><td>312.6</td></tr>
<tr><td>12</td><td>12</td><td>306.6</td></tr>
<tr><td>13</td><td>12.5</td><td>332.2</td></tr>
<tr><td>14</td><td>13</td><td>332.8</td></tr>
<tr><td>15</td><td>13.5</td><td>333.6</td></tr>
<tr><td>16</td><td rowspan="10">12.5</td><td>100</td><td>286.6</td></tr>
<tr><td>17</td><td>150</td><td>319.8</td></tr>
<tr><td>18</td><td>200</td><td>325.2</td></tr>
<tr><td>19</td><td>250</td><td>327.4</td></tr>
<tr><td>20</td><td>300</td><td>339.6</td></tr>
<tr><td>21</td><td rowspan="5">150</td><td>0.3</td><td>351.4</td></tr>
<tr><td>22</td><td>0.5</td><td>329.8</td></tr>
<tr><td>23</td><td>0.7</td><td>311.8</td></tr>
<tr><td>24</td><td>0.9</td><td>320.2</td></tr>
<tr><td>25</td><td>1.1</td><td>329.8</td></tr>
</table>

Then, the Taguchi method will be applied to evaluate the interaction of the input parameters, specifically, the parameters in the Taguchi method experiment are shown in **Table 5**. Both tables use five input levels for each parameter shown in **Table 3**.

Hardness test process

Before arc quenching, the convex samples are annealed at 600ºC for 30 min to remove the residual stress and achieve a stable structure. The reason is that the samples are deformed from a flat shape to a convex shape before heat treatment, creating residual stress within the sample. To measure the surface hardness of the hardened samples, this study used using an HR-150A Rockwell hardness tester (Yisite, Shenzhen, China). The surface hardness of the steel sample before annealing is 89.5 HRB. After annealing at 600ºC for 30 min, the sample reduces its hardness to 87.6 HRB, which is about 182 HV.
In addition, to measure the microhardness of the specimens, a Vickers hardness tester (HV) HM101 (Mitutoyo, Tokyo, Japan) was used after the specimens were cut using a wire electric discharge machine. Moreover, the microstructure of the hardened samples is observed via a microscope named Oxion OX.2153-PLM EUROMEX (Duiven, The Netherlands) and the scanning electron microscope (SEM) named JEOL 5410 LV (Tokyo, Japan).

RESULTS AND DISCUSSION

Univariate investigation method

After the quenching process, as shown in **Table 4**, the surface steel's hardness could improve to more than 300 HV, indicating a strong enhancement in the hardness quality. The following figures will further analyze the effects of each parameter on the hardness of the convex surface.
Fig. 2 depicts the influence of current intensity on the hardness of convex surface steel following arc quenching. The surface hardness of the specimens was 351.6 HV, 373.4 HV, 378.6 HV, 344.6 HV, and 343.4 HV at current intensities of 90 A, 100 A, 110 A, 120 A, and 130 A, respectively. The hardness of the specimens changed greatly when the Cr-I was increased from 90 A to 130 A. The reason for this change is that the heat input from the TIG gun is proportional to the Cr-I. In addition, there were two stages when the Cr-I was changed. Firstly, the hardness of surface steel increased from 351.6 HV to a maximum value of 378.6 HV when the current increased from 90 A to 110 A. The reason for this improvement may be that the heat process increased due to the increased current [23], which would result in a higher temperature of the steel surface.

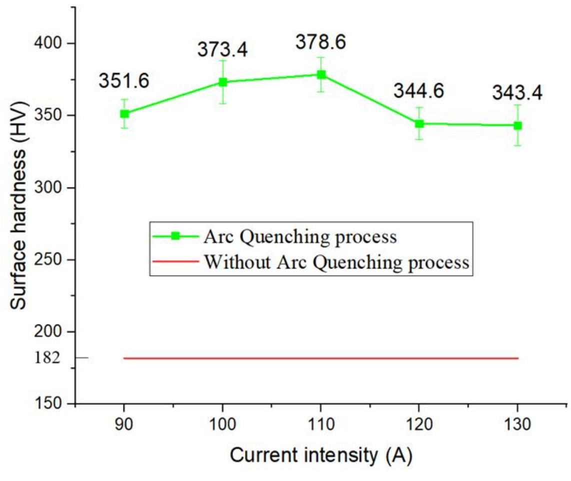

Fig. 2 Effects of current intensity on the hardness of convex surface steel after arc quenching.

At higher temperatures, the transformation of ferrite and pearlite phases to austenite phases occurs at a higher rate (higher temperatures produce more austenite grains) as the sample is heated further. Thus, the faster self-cooling of the material itself produces more martensite hard phases, which would increase the surface hardness. Compared to the initial hardness of 182 HV, the convex surface has an impressive increase of 108%. In the second stage, when the Cr-I increased from 110A to 130A, the surface hardness decreased from 344.6 HV at 120 A to 343.4 HV at 130 A. According to the study of Goyal et al. [24], the Cr-I is one of the factors affecting the heat input of the TIG technique. When the temperature becomes too high, the austenite grains tend to be coarser, leading to the formation of coarser martensite upon cooling. At that time, the coarse martensite grains will have a lower hardness than the fine-hardness martensite grains. In addition, when the temperature is too high, the oxidation process will occur more strongly, thereby reducing the surface hardness. Therefore, understanding and controlling the Cr-I is mandatory in the arc quenching process on the surface of S45C steel.
Fig. 3 depicts the impact of arc length on the hardness of the convex surface following arc quenching. The surface hardness of the samples was 365.2 HV, 332.2 HV, 321.8 HV, 300.6 HV, and 309.6 HV corresponding to Ar-Ls of 1.0 mm, 1.5 mm, 2.0 mm, 2.5 mm, and 3.0 mm, respectively. The results indicate that increasing the Ar-L mainly leads to a decrease in surface hardness. This was explained by Kumar et al. [18] that when the TIG tip is too high, it reduces the distribution of magnetic flux during heating to the steel surface. Lower surface temperature reduces the austenite phase, so after self-cooling, the proportion of the martensite phase appears lower, resulting in lower surface hardness. If the Ar-L is lower than 1.0 mm, the electrode is likely to stick to the steel surface, leading to the risk of electrode damage and interruption of the surface quenching process. Suppose the Ar-L is higher than 3.0 mm. In that case, it becomes more difficult to maintain a stable electric arc because the distance is quite large, reducing the amount of heat applied to the steel surface, thus also falsifying the martensite phase ratio. From this result, we can see that the optimal distance to achieve the maximum hardness is 1-2 mm. Adjusting the arc distance within this range enhances the efficiency of the steel surface quenching process, which will improve the wear resistance and the strength of the convex S45C steel surface. This is an important and easily controlled factor in production, helping to optimize product quality in arc quenching applications.

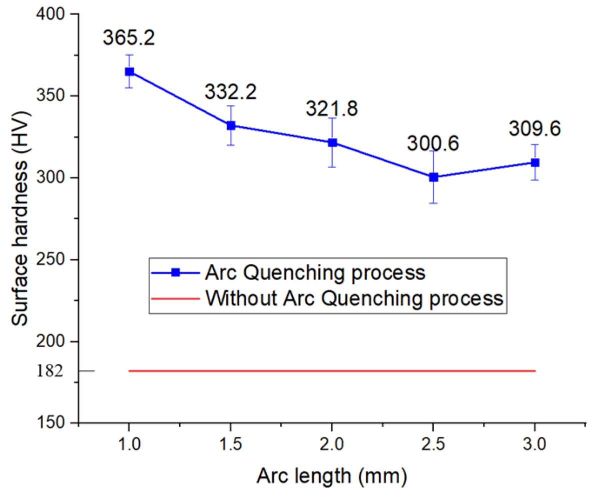

Fig. 3 Effects of arc length on the hardness of convex surface steel after arc quenching.

Fig. 4 shows the effects of gas flow rate on the hardness of convex surface steel after arc quenching. The surface hardness of the samples is 312.6 HV, 306.6 HV, 332.2 HV, 332.8 HV, and 333.6 HV corresponding to the GFR of 11.5, 12, 12.5, 13, and 13.5 l/min. In contrast to the Ar-L, increasing gas flow mainly increases the hardness of the surface. The cause for this hardness improvement is the better cooling rate of the gas. However, the changing rate is not high, and the surface hardness mostly oscillates around 320 HV. This is also explained by the fact that when the GFR increases, it will remove a specific quantity of heat created by the TIG tip. So, increasing the gas flow is not very meaningful when it has the opposite effect in the process of quenching. In addition, high gas flow will cause waste and increase production costs. In industrial applications, ensuring the appropriate air flow is something that engineers need to consider. Moderate air flow will be suitable for ensuring a full surface hardening process while still achieving optimal hardness. If the gas flow is too high, it will reduce the efficiency of surface heating energy and increase costs, which is not suitable for mass production.

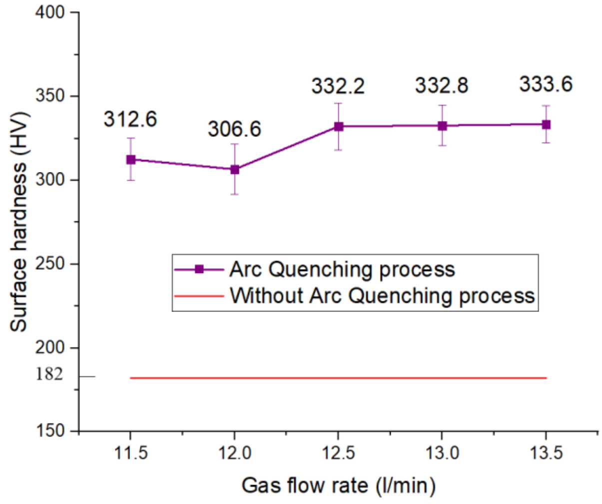

Fig. 4 Effects of gas flow rate on the hardness of convex surface steel after arc quenching.

Tr-S has a direct impact on heat input during quenching, as well as microstructure and surface hardness [24]. Fig 5 shows the effect of Tr-S on the hardness of convex surface steel after arc quenching. The results show that when the Tr-S increases from 100 mm/min to 300 mm/min, the surface hardness increases from 286.6 HV to 339.8 HV. At travel speeds below 100 mm/min, the TIG head travel is slower, so the heating time for the surface is longer, leading to excessive heat input, affecting the grain structure after quenching (coarser grain) and thus reducing the hardness of the surface steel. When the Tr-S rises from 150-250 mm/min, the heat input decreases, minimizing overheating and promoting the formation of finer martensitic structures, which increases the hardness (the curve tends to be horizontal) from 319.8 HV - 327.4 HV. At 300 mm/min, the hardness of the surface steel after quenching process is at 339.8 HV, the increase graph tends to increase by about 150 -250 mm/min, but according to [18], the material surface will not absorb enough heat needed for the quenching process when moving too fast, which will reduce the phase transformation efficiency, which can be seen as the surface is unstable, and will be re-examined in the Taguchi analysis for verification. Therefore, choosing the appropriate Tr-S is essential to balance the heat input and the rapid cooling rate to obtain optimal hardness. If the speed is too slow, overheating will result in coarser grains and lower hardness, while too high a speed may prevent sufficient heating for martensitic transformation.

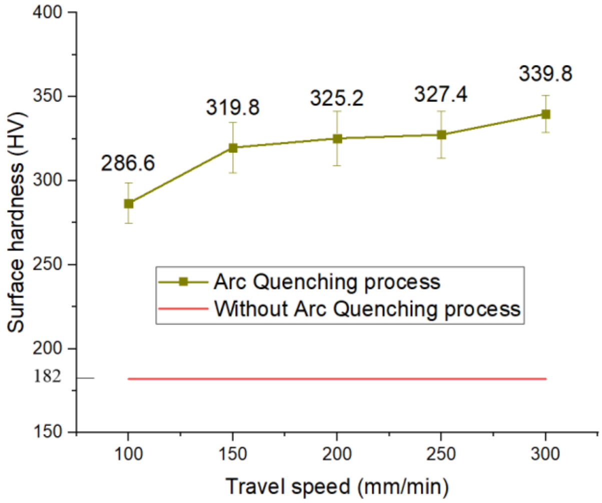

Fig. 5 Effects of travel speed on the hardness of convex surface steel after arc quenching.

Pulse duration has a direct impact on the quantity of heat created at the TIG tip [24]. **Fig. 6** shows the effect of T_{on} on the hardness of convex surface steel after surface quenching by an electric arc. The experiment was carried out with different pulse durations of 0.3 s, 0.5 s, 0.7 s, 0.9 s, and 1.1 s combined with a pulse rest time T_{off} of 0.1 s between each T_{on} to decrease the amount of heat created at the TIG tip [24]. The surface hardness at 0.3 s pulse duration was 351.4 HV, at 0.5 s it was 329.8 HV, at 0.7 s it was 311.8 HV, at 0.9 s it was 320.2 HV and at 1.1 s it was 329.8 HV. Obviously, the highest hardness (351.4 HV) was achieved at Ton = 0.3 s, when the heat released was lower than at other pulse values and the amount of heat absorbed into the surface was within the optimal range. As T_{on} increased from 0.3 s to 0.7 s, the hardness tended to decrease to 311.8 HV, which can be explained by the fact that the increased heat input reduced the efficiency of the rapid self-cooling process of the part itself. However, after 0.7 s, the hardness increased again, reaching 329.8 HV at 1.1 s, which could be attributed to a stable heat transfer mechanism caused by the T_{off} cycle being adjusted to 0.1 s, allowing for a more optimum grain structure after quenching. These findings will shed light on industrial electric arc quenching applications, where pulse parameter management can improve wear resistance and extend the service life of S45C steel components.

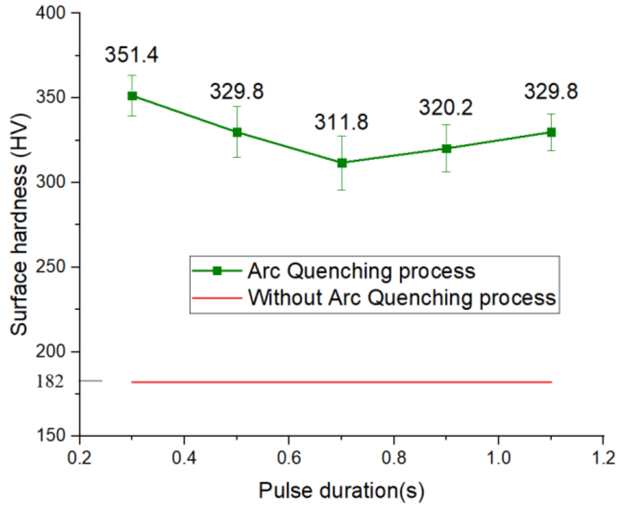

Fig. 6 Effects of T_{on} on the hardness of convex surface steel after arc quenching.

Taguchi method

Table 5 shows the Taguchi-designed experiment parameters for arc quenching using convex surface samples. The 7th column of Table 5 was the result of average surface hardness (HV). According to this column, the highest hardness value reaches 355.0 HV corresponding to the parameters was 90 A for the Cr-I, 2 mm for the Ar-L, 12.5 l/min for the GFR, 200 mm/min for the Tr-S, and 0.7 s for the T_{on}.

Table 6 shows the Response Table for Means of the hardness of the convex surface with “larger is better” criteria. Cr-I has the greatest impact on the surface hardness of steel. Second is the Tr-S of the TIG head, third is the T_{on} parameter. These parameters directly and strongly impact the heat source of the arc TIG [25]. The lesser impact on surface hardness is Ar-L and GFR, which ranked fourth and fifth, respectively.

Fig. 7 shows the Main effects plot for Means of the hardness of the convex surface steel with “larger is better” criteria. In this graph, the optimal values of the parameter are noted at the peaks of the graph. With the peak system, the ideal parameters are the Cr-I of 90 A, Ar-L of 2.5 mm, GFR of 12 l/min, Tr-S of 200 mm/min, and Ton of 0.7 s. Taguchi prediction value of the convex surface hardness is 359.6 HV, which is slightly higher than the maximum value of **Table 5,** indicating the possibility of further improvement of the surface hardness.

Table 5 Experiment settings designed using the Taguchi method for arc quenching with convex surface samples

No.	Intensity (A)	Arc length (mm)	Q (l/min)	F (mm/min)	Pulse duration (s)	Average Surface hardness (HV)
1	90	1	11.5	100	0.3	289.4
2	90	1.5	12	150	0.5	323.0
3	90	2	12.5	200	0.7	355.0
4	90	2.5	13	250	0.9	354.2
5	90	3	13.5	300	1.1	308.2
6	100	1	12	200	0.9	309.0
7	100	1.5	12.5	250	1.1	302.4
8	100	2	13	300	0.3	278.6
9	100	2.5	13.5	100	0.5	294.6
10	100	3	11.5	150	0.7	277.2
11	110	1	12.5	300	0.5	289.4
12	110	1.5	13	100	0.7	304.0
13	110	2	13.5	150	0.9	295.2
14	110	2.5	11.5	200	1.1	295.6
15	110	3	12	250	0.3	301.8
16	120	1	13	150	1.1	280.2
17	120	1.5	13.5	200	0.3	310.4
18	120	2	11.5	250	0.5	311.2
19	120	2.5	12	300	0.7	321.2
20	120	3	12.5	100	0.9	289.4
21	130	1	13.5	250	0.7	283.2
22	130	1.5	11.5	300	0.9	293.0
23	130	2	12	100	1.1	288.6
24	130	2.5	12.5	150	0.3	272.8
25	130	3	13	200	0.5	288.2

Table 6 Taguchi results of response table for means of the hardness with the convex surface steel (larger is better).

Level	Intensity	Arc length	Gas flow rate	Travel speed	Pulse duration
1	326.0	290.2	293.3	293.2	290.6
2	292.4	306.6	308.7	289.7	301.3
3	297.2	305.7	301.8	311.6	308.1
4	302.5	307.7	301.0	310.6	308.2
5	285.2	293.0	298.3	298.1	295.0
Delta	40.8	17.4	15.4	22.0	17.6
Rank	1	4	5	2	3

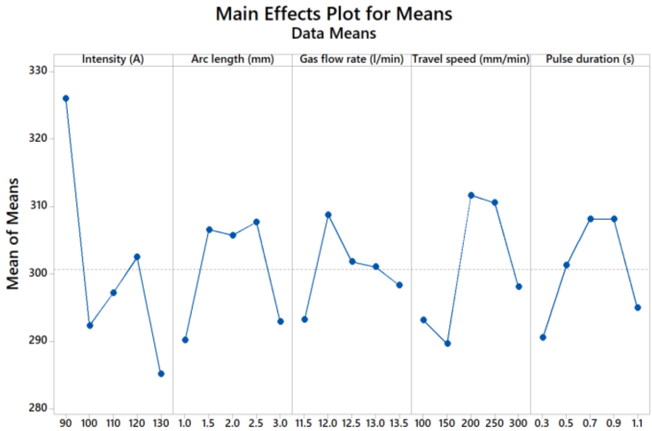

Fig. 7 Main effects plot for the Means of the hardness of the convex surface steel (larger is better).

The results of the interaction analysis of the mean values of average surface hardness (HV) are shown in **Fig. 8**. The graph confirms that the parameters have a significant influence on the HV, as indicated by the non-parallel lines. This further proves that the hardness of the S45C steel surface after quenching depends on many parameters, and they are useful for studying to improve the hardness of the surface steel.

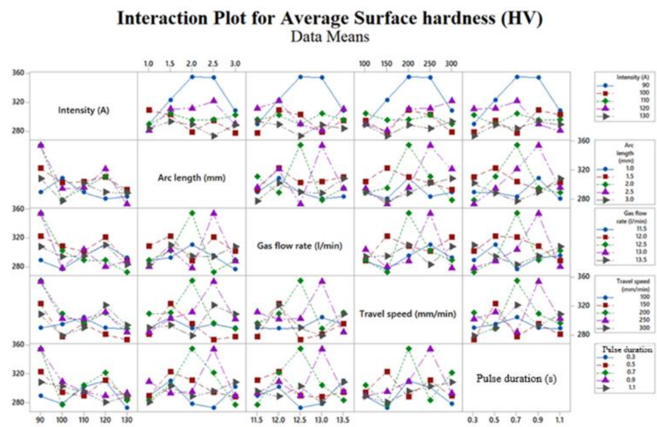

Fig. 8 The interaction plot for mean of average surface hardness

The 3D surface plots analysis

Fig. 9a shows a 3D surface plot depicting the simultaneous effect of Cr-I and Ar-L on surface hardness. In **Fig. 9a**, the intensity has affected the surface hardness values more than the Ar-L. This is explained by the fact that Cr-I is the main factor that strongly affects the heat input of the TIG process [24]. The optimum surface hardness value (the highest peak position of the 3D surface graph) is obtained at an intensity of 90 A, with the Ar-L at 2 mm. The position with the second-highest peak of this graph is when the current is at 90 A and the Ar-L is 2.5 mm. It can be seen that the optimum Ar-L is between 2 mm and 2.5 mm. **Fig. 9b** shows the surface hardness, intensity, and GFR relationship. The optimum surface hardness value is obtained at an intensity of 90 A, with GFR at 12.5 l/min. The position with the second-highest peak in this graph is when the current is at 90 A and GFR is 13 l/min. This shows that the GFR has a lower effect on the surface hardness than the Cr-I. **Fig. 10a** shows a 3D surface plot depicting the simultaneous effect of current intensity, and Tr-S on surface hardness. In **Fig. 10a**, the same thing happens when the Cr-I has a stronger influence than the Tr-S. When the Tr-S increases, the hardness of the surface steel after quenching process has a clearer change according to the rule at all levels of Cr-I. The optimum surface hardness value is achieved at 90 A (current intensity), and 200 mm/min (Tr-S). The position with the second highest peak of this graph is when the current is achieved at 90 A (current intensity), and 250 mm/min

(Tr-S). **Fig 10b** shows the relationship between Cr-I and pulse duration to the hardness of the convex surface steel. These two parameters are closely related to each other and are related to the heat generation process at the TIG tip [24]. Similar to Fig. 9 and Fig. 10a, increasing Cr-I will reduce hardness. The ideal interaction range and the clearer trend of pulse duration are from 0.7s to 0.9s; from 0.3s to 0.7s, the stability is not high. The optimum Surface hardness value is obtained at an intensity of 90 A, with Ton at 0.7 s. The position with the second-highest peak of this graph is when the current is at 90 A and Ton is 0.9 s. This shows that Ton has a lower effect on the surface hardness than the current intensity. **Fig. 11a** shows the relationship between the hardness of the steel surface after quenching for the two parameters T_{on} and Ar-L. When considering the TIG Ar-L parameter in between 1.5 mm and 2.5 mm (good value range as analyzed in **Fig. 9a**). The optimal value is achieved at the position with 2 mm for Ar-L and 0.7 s for T_{on}. This is similar to the optimal values of T_{on} at 0.7 s in **Fig 10b** and Ar-L at 2 mm shown in **Fig 9a**. The position with the second highest peak of this graph is when Ar-L is at 2.5 (mm) and T_{on} is 0.9 (s). The relationship between the surface hardness of the S45C steel after quenching for the two parameters T_{on} and GFR is shown in Fig 11b. The optimal value is achieved at the position with a GFR of 12.5 l/min and 0.7 s for T_{on}. This is similar to the optimal values of T_{on} at 0.7 s in Figs 10b and 11a; and 12.5 (l/min) for GFR shown in **Fig 9b**. The position with the second highest peak of this graph is when GFR is at 13 l/min and T_{on} is 0.9 s. **Fig 12a** shows the effects of the two parameters Ar-L and Tr-S on the hardness of the surface after quenching. The optimal value is achieved at the position with a Tr-S of 200 mm/min and 2 mm for Ar-L. This is similar to the optimal values of Tr-S at 200 (mm/min) in **Fig. 10a** and Ar-L at 12.5 (l/min) shown in **Figs 9a** and **11a**. The position with the second highest peak of this graph is when the Tr-S is at 250 mm/min and the Ar-L is 2.5 mm. These are the positions where there is a strong interaction between the two parameters: movement the Tr-S and the Ar-L. **Fig 12b** shows the effects of the two parameters T_{on} and travel speed on the hardness of the surface after quenching. The optimal value is achieved at the position with 200 mm/min for Tr-S and 0.7 s for T_{on}. This is similar to the optimal values of Tr-S at 200 mm/min in **Figs 10a, 12a,** and T_{on} at 0.7 s shown in **Figs 10b, 11**. The position with the second highest peak of this graph is when Tr-S is at 250 (mm/min) and T_{on} is 0.9 s. These are the positions where there is a strong interaction between the two parameters: movement Tr-S and T_{on}. **Fig. 13a** shows the interaction between the two parameters Tr-S and GFR on the surface hardness of the steel after quenching. The optimum value is obtained at the position with 12.5 l/min (GFR) and 200 mm/min (Tr-S). This is similar to the optimal values **Figs 10a and 12** for Tr-S; in **Figs 9b, and 11b** for GFR. The position with the second highest peak of this graph is when Tr-S is at 250 (mm/min) and GFR is 13 (l/min). These are the positions where there is a strong interaction between the two parameters: movement Tr-S and GFR. **Fig. 13b** shows the relationship between the hardness of the steel surface after quenching for the two parameters Ar-L and GFR. The best value is achieved at the position at 2 mm (Ar-L) and 12.5 l/min (GFR). This result is similar **Figs 9a, 11a, and 12a** for Ar-L; **Figs 9b, 11b, and 13a** the GFR. The position with the second highest peak of this graph is when the Ar-L is at 2.5 mm and the GFR is 13 l/min. These are the positions where there is a strong interaction between the two parameters: movement, GFR, and Ar-L.

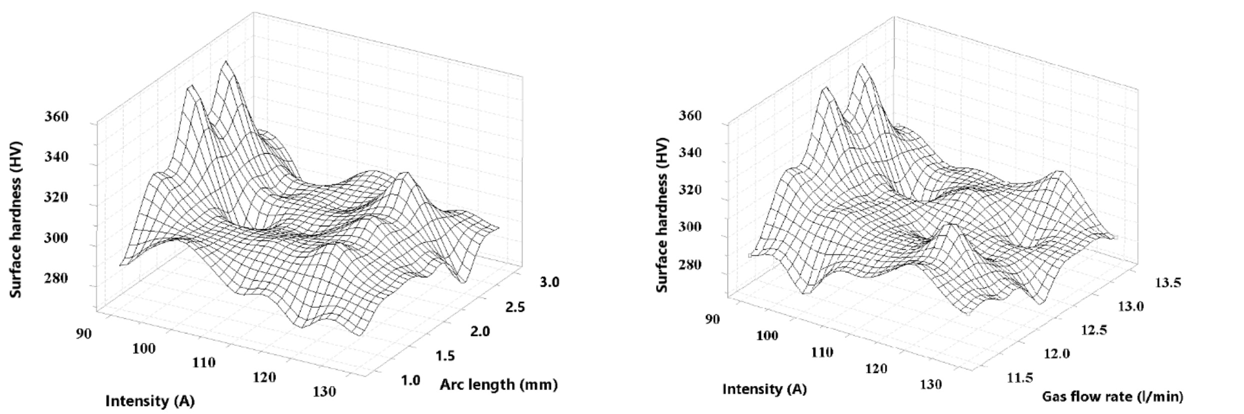

(a) (b)

Fig. 9 The 3D surface graph illustrates the relationship between intensity, arc length, and gas flow rate on steel surface hardness following the arc quenching process: (a) Current intensity and arc length, (b) Current intensity and gas flow rate

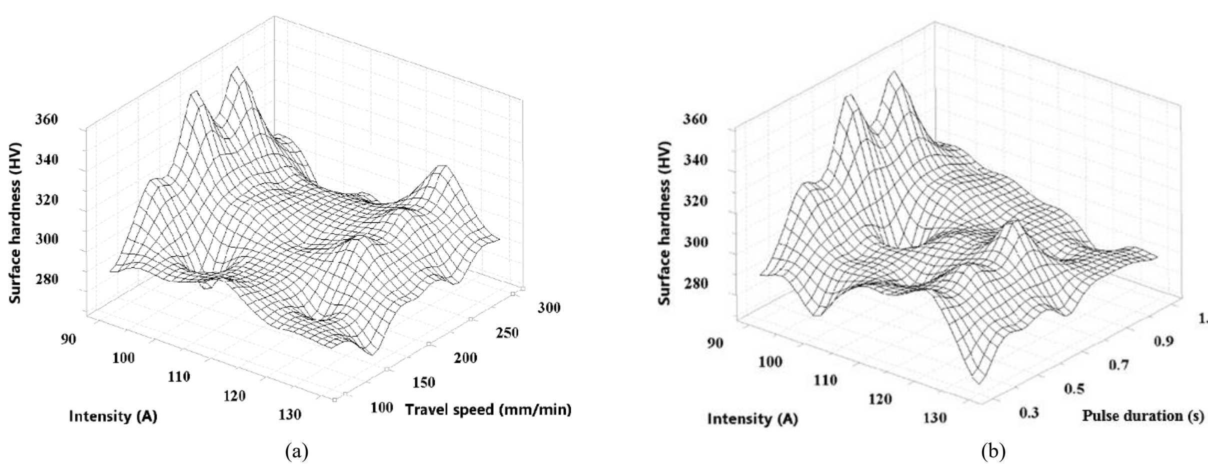

(a) (b)

Fig. 10 The 3D surface graph illustrates the relationship between current intensity, travel speed and T_{on} on steel surface hardness following arc quenching process: (a) Current intensity and Travel speed, (b) Current intensity and T_{on}

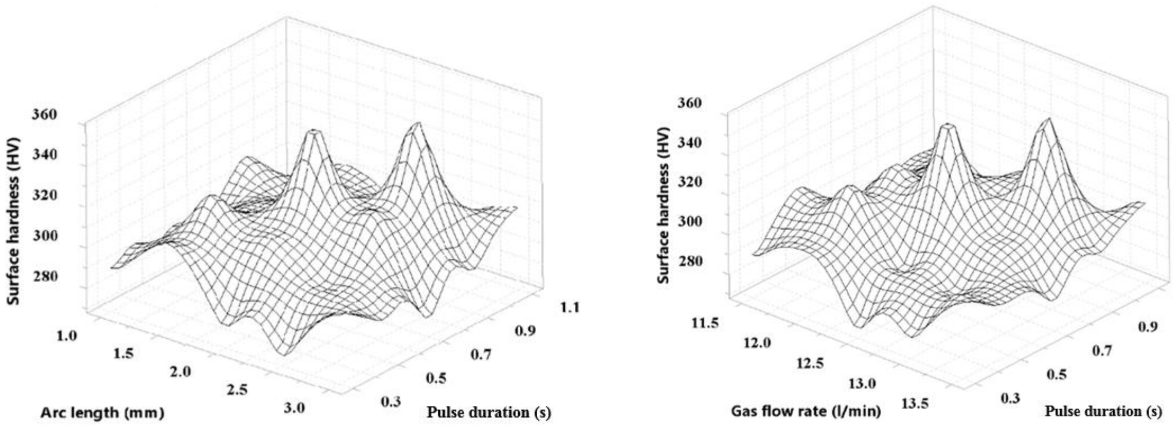

(a) (b)

Fig. 11 The 3D surface graph illustrates the relationship between Arc length, Gas flow rate and T_{on} on steel surface hardness following arc quenching process: (a) T_{on} and Arc length, (b) Gas flow and T_{on}.

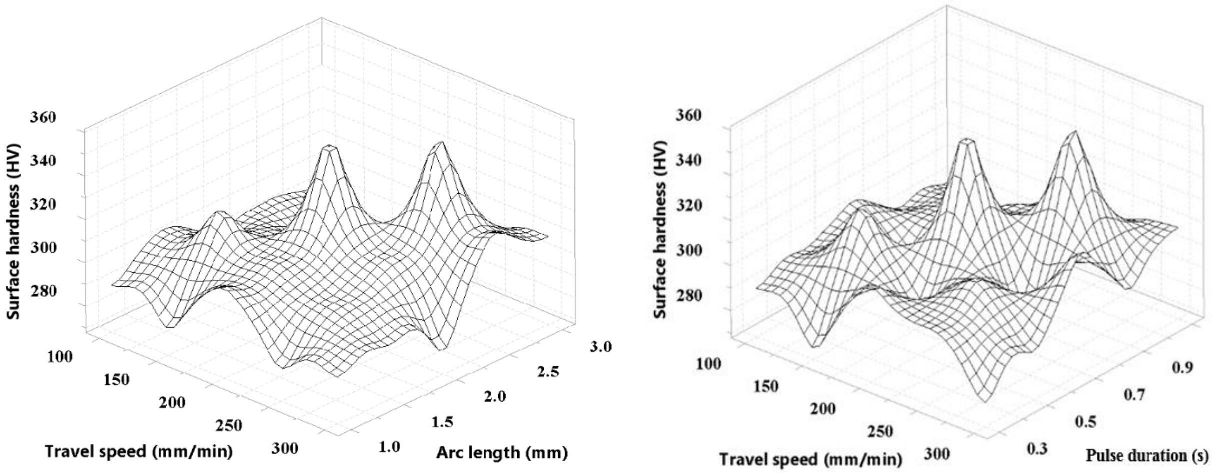

(a) (b)

Fig. 12 The 3D surface graph illustrates the relationship between T_{on}, Travel speed and Arc length on steel surface hardness following arc quenching process: (a) Travel speed and Arc length, (b) Travel speed and T_{on}.

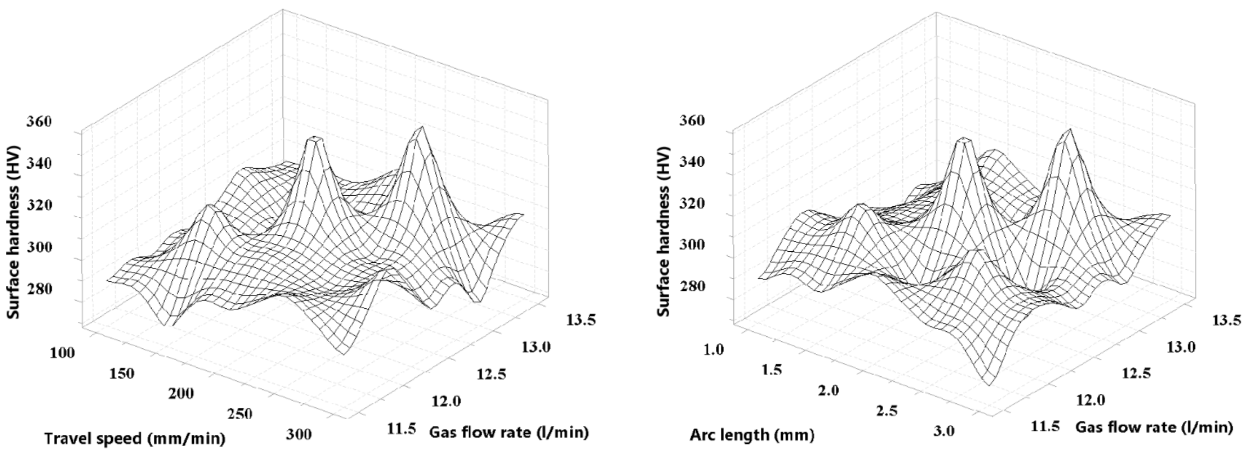

(a) (b)

Fig. 13 The 3D surface graph illustrates the relationship between Gas flow rate, Travel speed and Arc length on steel surface hardness following arc quenching process: (a) Gas flow rate and Travel speed, (b) Arc length and Gas flow rate

Microstructure and microhardness analysis

Fig. 14 shows the results of microstructure observations of the steel sample after quenching. There are three zones in the samples: the hardening zone, the heat-affected zone, and the base zone [18]. The base zone (**Fig. 14d**) was an unheated area with ferrite and pearlite phases [16]. The grain structure for this original structure has a large and coarse plate morphology, which is due to the slow cooling process caused by the annealing treatment of the steel [6]. The heat-affected zone is located between the hardened zone and the base zone; according to [26], the bainite phase may appear in this area, in addition to the two basic phases of ferrite and pearlite, a small amount of martensite phase also exists. Therefore, this area will have higher hardness than the area with the original structure after annealing of S45C steel. Finally, the hardened zone (**Fig. 14b**) with the highest hardness in the center of the quenched sample has a martensite phase interspersed with remaining austenite [27]. It can be seen that the grain microstructure in this area is very fine; this is due to the very rapid cooling process [6]. When observing the microstructure under a scanning electron microscope, the martensite phase has a needle shape along the cooling direction as shown in **Fig. 14c**. It is this phase that increases the hardness of the S45C steel material. In addition, according to **Fig. 14a**, the hard zone may have melted and created a moving flow, resulting in many longitudinal marks [28]. This is explained by the heating process with a large amount of heat emitted from the TIG tip with a temperature of about 1140ºC -1500ºC [13]. Sample No. 3 of **Table 3** was selected to test the microhardness in depth of the three surface areas of the sample, and **Fig. 15** is the result. Despite the fluctuation in the diagram, the microhardness mostly declines from 332 HV to 219 HV when the depth increases from 100 µm to 3500 µm. The high-hardness layer thickness value is 2000 µm, which is better than the studies of E N Safonov et al [14, 15, 17]. In study [14], only the depth of the hard zone from 0.5-0.9mm was achieved; study [15] only achieved the maximum depth of the high hardness layer of 1200 µm; and study [17] only attained the depth of the hardening zone at 0.7-1mm. The original hardness of the sample is 182 HV, therefore, the case depth could be higher than 3500 µm.

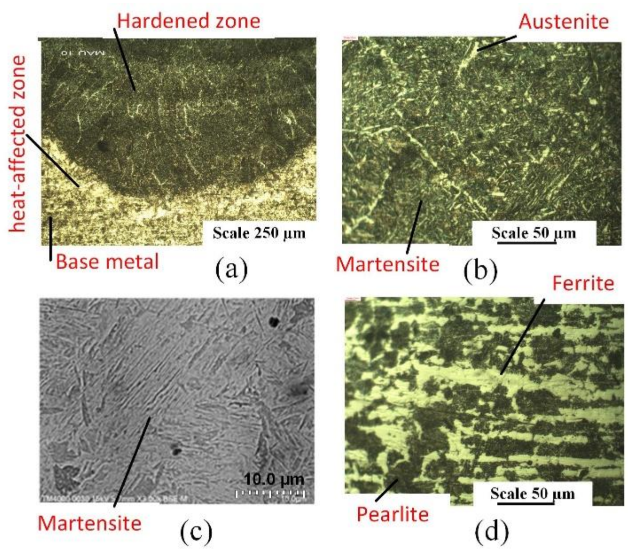

Fig. 14 Microstructure of the S45C steel sample with convex surface: (a) overview of the quenched area, (b) and (c) Martensite and austenite structures of the hardening zone, (d) perlitic and ferritic phases of the base metal.

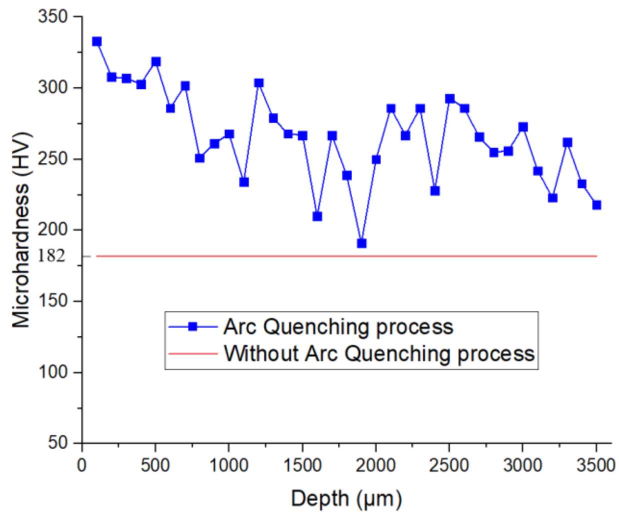

Fig. 15 Hardness of sample No. 3 according to the micro depth of the cross section

CONCLUSION

This study examined many factors affecting the surface hardness of S45C steel material after quenching such as pulse duration, gas flow rate, current intensity, travel speed and arc length. The findings of this work are summarized below:

- The current intensity most strongly influences the surface hardness. The second is Travel speed, and the T_{on} specification comes in third. The arc length and the gas flow rate are ranked for the fourth and fifth places, respectively.
- In contrast to its initial hardness of 182 HV, the convex surface exhibits a remarkable 108% rising percentage. The overheating and melting phenomena as well as the decreased hardness could result from an excessively high heat input at a high current intensity.
- Arc length increases primarily and result in a decrease in surface hardness, which a drop in surface temperature may bring on. Increases in gas flow rate mainly leads to increasing surface hardness in the opposite direction of the arc length. The improved gas cooling rate is the cause of this hardness improvement. Surface hardness increases as the TIG gun's travel speed does, much like the gas flow rate does. The decrease in overheating is the cause of the increased surface hardness with increasing travel speed.
- Taguchi prediction value of the convex surface hardness is 359.6 HV, with optimal parameters are the current intensity of 90 A, the arc length of 2.5 mm, the gas flow rate of 12 l/min, the travel speed of 200 mm/min, and the T_{on} of 0.7 s.
- The analysis of the interaction between the parameters is shown through the 3D surface graphs. All these graphs show the optimal values with the current intensity at 90 A, the travel speed at 200 mm/min, the arc length at 2 mm, the gas flow rate at 12.5 l/min and finally the T_{on} at 0.7 s.
- The maximum case depth of the arc quenching for S45C convex surface is 3500 µm. There are three areas in the microstructure of the arc quenching sample: hardened area, heat-affected area, and the base substrate.

Acknowledgements: The authors acknowledge the funding from HCMC University of Technology and Education under grant number T2024-29 for this study

REFERENCES

1. P.P.K. Reddy, et al. Journal of The Institution of Engineers (India): Series D, 2024. https://doi.org/10.1007/s40033-024-00714-8

2. Chen, Z., Zhu, Q., Wang, J., Yun, X., He, B., & Luo, J. Optics & Laser Technology, 103, 2018, 118-125. https://doi.org/10.1016/j.optlastec.2018.01.039
3. Schneider, J. M., Timken, C., & Chatterjee, S. M. *Steel Heat Treating Fundamentals and Processes*. ASM Handbook, 4, 2013, 390-398.
4. Dewangan, S., Mainwal, N., Khandelwal, M., & Jadhav, P. S. Australian Journal of Mechanical Engineering, 20(1), 74–87. https://doi.org/10.1080/14484846.2019.1664212
5. Q. Jiang, S. Wang: Journal of Physics: Conference Series, 2713, 2024, 012056. https://doi.org/10.1088/1742-6596/2713/1/012056
6. A.R. Kulkarni, T. Kukreja, S. Dewangan: Acta Metallurgica Slovaca, 31(2), 2025, 101–107. https://doi.org/10.36547/ams.31.2.2176
7. Colombini, E., Sola, R., Parigi, G., Veronesi, P., & Poli, G. Metallurgical and Materials Transactions A, 45, 2014, 5562-5573. https://doi.org/10.1007/s11661-014-2490-z
8. Lee, M. K., Kim, G. H., Kim, K. H., Kim, W. W. Surface and Coatings Technology, 184(2-3), 2004, 239-246. https://doi.org/10.1016/j.surfcoat.2003.10.063
9. Śliwiński, P., Kubik, K., Kopyścianski, M. Low-Alloy Steel Electron Beam Hardening. *Proceedings 31st International Conference on Metallurgy and Materials*, Brno, Czech Republic, 2022, 382-387. https://doi.org/10.37904/metal.2022.4411
10. Purwanto, H. et al. IOP Conference Series: Materials Science and Engineering, 694, 2019, 012041. https://doi.org/10.1088/1757-899X/694/1/012041
11. Safonov, E. N., Zhuravlev, V. I. Welding International, 12(4), 1998, 326-328. https://doi.org/10.1080/09507119809448495
12. Mikheev, A.E.., Ivasev, S.S., Girn, A.V., Terekhin, N.A., Statsura, V.V. Welding International, 17(7), 2003, 570-572. https://doi.org/10.1533/wint.2003.3162
13. S. Kumar, P.K. Ghosh, R. Kumar: Journal of Materials Processing Technology, 249, 2017, 394-406. https://doi.org/10.1016/j.jmatprotec.2017.06.035
14. E.N. Safonov: Structure and Hardness of Cast Iron after Surface Hardening. Metal Science and Heat Treatment, 47, 2005, 434–439. https://doi.org/10.1007/s11041-006-0007-0
15. E.N. Safonov: IOP Conference Series: Materials Science and Engineering, 966, 2020, 012066. https://doi.org/10.1088/1757-899X/966/1/012066
16. S. Kumar, P.K Ghosh: International Journal of Fatigue, 116, 2018, 306-316. https://doi.org/10.1016/j.ijfatigue.2018.06.036
17. E.N. Safonov, M.V. Mironova: Materials Science Forum, 989, 2020, 318-323. https://doi.org/10.4028/www.scientific.net/MSF.989.318
18. R. Kumar, P.K. Ghosh, S. Kumar: Journal of Materials Processing Technology, 240, 2017, 420-431. https://doi.org/10.1016/j.jmatprotec.2016.10.020
19. S. Dewangan, V.V. Nemade, K.H. Nemade: Acta Metallurgica Slovaca, 29(1), 2023, 26–33. https://doi.org/10.36547/ams.29.1.1719
20. Joshi, J., Sahu, S. K. Experimental Heat Transfer, 35(7), 2021, 938–963. https://doi.org/10.1080/08916152.2021.1995082
21. Dong Ju Kim, Seyeong Jeong, Tongil Park, Daegyoum Kim. International Journal of Heat and Fluid Flow, 79, 2019, 108458. https://doi.org/10.1016/j.ijheatfluidflow.2019.108458
22. Meyghani, B., Awang, M. Archives of Computational Methods in Engineering, 27, 2020, 563–576. https://doi.org/10.1007/s11831-019-09319-x
23. Nguyen, N. et al. Welding Journal, 1999, 265s-274s.
24. V.K. Goyal, P.K. Ghosh, J.S. Saini: Journal of Materials Processing Technology, 209, 2009, 1318–1336. https://doi.org/10.1016/j.jmatprotec.2008.03.035
25. Uyen, T.M.T.; Minh, P.S.; Nguyen, V.T.; Do, T.T.; Nguyen, V.T.; Le, M.T.; Nguyen, V.T.T. Micromachines, 14, 2023, 827. https://doi.org/10.3390/mi14040827
26. Zhang, G.; Xiong, J.; Gao, H.; Wu, L. Journal of Quantitative Spectroscopy and Radiative Transfer, 113(15), 2012, 1938-1945. https://doi.org/10.1016/j.jqsrt.2012.05.018
27. Ghosh, P.K., Kumar, R. Metallurgical and Materials Transactions A, 46, 2015, 831–842. https://doi.org/10.1007/s11661-014-2670-x
28. V.A. Hosseini, L. Karlsson, K. Hurtig, I. Choquet, D. Engelberg, M.J. Roy, Ch. Kumara: Materials & Design, 121, 2017, 11-23. https://doi.org/10.1016/j.matdes.2017.02.042